Inverse Radiative Problem in Semitransparent Slab with Variable Spatial Refractive Index

L. H. Liu*
Harbin Institute of Technology,
150001 Harbin, People's Republic of China

I. Introduction

THE inverse analysis of radiation in a participating medium has a broad range of engineering applications, for example, determination of the radiative properties of a medium, prediction of temperature distribution in a flame, and analysis of fiber-optic cables with radially varying refractive indices. Inverse radiation problems that deal with the prediction of the source term or the temperature distribution in semitransparent media from radiation measurements have been reported by many researchers. Li and Ozisik,[1] Siewert,[2,3] Li,[4–6] and Liu et al.[7–9] have reconstructed the temperature profiles or source terms in plane-parallel, spherical, cylindrical, and rectangular media by inverse analysis. Yousefian and Lallemand,[10] Yousefian et al.,[11] Solomon et al.,[12] and Best et al.[13] determined the temperature and species concentration profiles of axisymmetric flames by emission and transmission infrared spectral measurements. Despite the relatively high interest that has been expressed in inverse radiation problems of the source term or the temperature distribution, most work has considered media with constant refractive indices.

Because of the structural characteristics of materials or possible temperature dependency, the refractive index of a medium may be a function of the spatial position. In this case, the rays propagating inside the medium are not straight lines. The effects of refractive index on radiative transfer have been noticed by some researchers. Siegel and Spuckler[14,15] studied radiative transfer in multilayer slabs of a semitransparent medium, in which the refractive index of a layer of the medium is constant and different from that of another layer of the medium. Ben Abdallah and Le Dez[16–19] developed and used a curved ray-tracing technique to analyze the radiative heat transfer in semitransparent medium with variable spatial refractive index. Liu[20] presented a discrete curved ray-tracing method for analyzing the radiative transfer in a semitransparent slab with variable spatial refractive index. Lemonnier and Le Dez[21] applied the discrete ordinates method to solve the radiative transfer across a slab with variable refractive index. Huang et al.[22,23] presented a combined curved ray-tracing and pseudo source-adding method for radiative transfer in a semitransparent slab with graded refractive index. Liu et al.[24] used a Monte Carlo curved ray-tracing method to analyze radiative transfer in a semitransparent slab with variable spatial refractive index. To the author's knowledge, no work has investigated the inverse radiative problem of source term in the medium with variable refractive index.

In this Note, we deal with the inverse radiation problem of finding the source term in a one-dimensional semitransparent slab with graded refractive index from the measured exit radiation intensities on the boundaries. A backward Monte Carlo curved ray-tracing method based on the radiation distribution factor is used to solve the radiative transfer equation. The inverse problem is solved using the conjugate gradient. The effects of the gradient of refractive index on the accuracy of the inverse analysis will be analyzed.

Received 11 October 2003; revision received 15 November 2003; accepted for publication 5 December 2003.

*Professor, School of Energy Science and Engineering, 92 West Dazhi Street; liulh_hit@263.net.

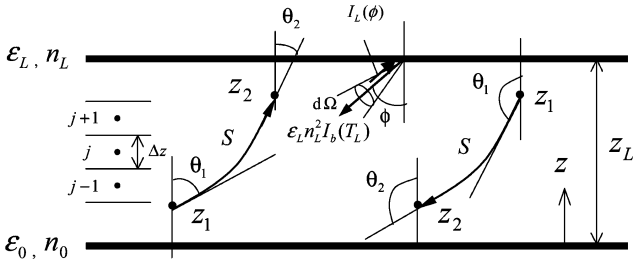

Fig. 1 Physical model and ray tracing.

II. Physical Model

As shown in Fig. 1, we consider a one-dimensional semitransparent gray absorbing–emitting slab with thickness z_L. The boundaries are opaque, diffuse, and gray walls. The emissivities of the boundary walls are ε_0 and ε_L at $z=0$ and $z=z_L$, respectively. The absorption coefficient k_a is uniform over the slab, but the refractive index n of the medium varies linearly with the axis coordinate z. The radiative transfer equation at steady state in an absorbing–emitting medium with spatially variable refractive index is given by

$$\frac{\mathrm{d}}{\mathrm{d}s}\left[\frac{I(s,\mu)}{n^2(s)}\right] + k_a(s)\frac{I(s,\mu)}{n^2(s)} = k_a(s) I_b[T(s)] \tag{1}$$

with boundary conditions

$$I_0(\mu) = \frac{\varepsilon_0 n_0^2 \sigma T_0^4}{\pi} + 2(1-\varepsilon_0)\int_{-1}^{0} I_0(\mu')\,\mu'\,\mathrm{d}\mu' \qquad \text{at} \quad z=0, \quad \mu>0 \tag{2a}$$

$$I_L(\mu) = \frac{\varepsilon_L n_L^2 \sigma T_L^4}{\pi} + 2(1-\varepsilon_L)\int_{0}^{1} I_L(\mu')\,\mu'\,\mathrm{d}\mu' \qquad \text{at} \quad z=z_L, \quad \mu<0 \tag{2b}$$

where $I(s,\mu)$ is the radiation intensity, s is the abscissa on the ray trajectory and is determined by the ray equation discussed in the following section, $\mu=\cos\theta$ is the direction cosine, and σ is the Stefen–Boltzmann constant. For the inverse radiation problems considered here, the source term is regarded as unknown, but the other quantities in Eqs. (1) and (2) are known. In addition, the measured exit radiation intensities at the boundaries and the temperatures of the boundaries are available. The source term is to be determined from the measured exit radiation intensities.

III. Backward Monte Carlo Curved Ray-Tracing Method

As shown in Fig. 1, in the case of $n_0<n_L$, if $\theta_1<\pi/2$, the curvilinear abscissa S on the ray trajectory from z_1 to z_2 is determined by the ray equation deduced from the Fermat principle, and can be written as[19]

$$S = [z_L/(n_L-n_0)]\left[\sqrt{n^2(z_2)-n^2(z_1)\sin^2\theta_1} - n(z_1)\cos\theta_1\right] \qquad \theta_1<\pi/2 \tag{3}$$

Similarly, if $\theta_1>\pi/2$ and $n(z_1)\sin\theta_1 \le n(z_2)$, the curvilinear abscissa S from z_1 to z_2 can be written as

$$S = -[z_L/(n_L-n_0)]\left[n(z_1)\cos\theta_1 + \sqrt{n^2(z_2)-n^2(z_1)\sin^2\theta_1}\right] \qquad n(z_1)\sin\theta_1 \le n(z_2) \tag{4}$$

If $\theta_1>\pi/2$ and $n(z_1)\sin\theta_1 = n(z_2)$, the ray is totally reflected back at z_2, and the curvilinear abscissa S on the ray trajectory from z_1 to z_2 can be expressed as

$$S = -\frac{z_L n(z_1)\cos\theta_1}{n_L-n_0}, \qquad n(z_1)\sin\theta_1 = n(z_2) \tag{5}$$

Backward Monte Carlo methods start at a termination site and trace the photon bundle in the reverse direction. Walters and Buckius[25] developed a comprehensive reverse Monte Carlo method for computing the emission of a generalized enclosure containing an absorbing, emitting, and scattering medium. Modest[26] gave a comprehensive formulation for backward Monte Carlo simulation, capable of treating emitting, absorbing, and anisotropically scattering media with collimated irradiation, point or line sources. Liu[27] developed a backward Monte Carlo method based on the concept of a radiation distribution factor. If the radiative properties of the medium and boundary do not depend on the temperature, the backward Monte Carlo method based on the concept of a radiation distribution factor is very efficient, especially for inverse analysis of a temperature field using outgoing emission intensity.

To deduce the formulas for the calculation of exit radiation intensity at boundaries, as shown in Fig. 1, the slab is divided into N sublayers. The radiant power emitted from the upper boundary surface in a solid angle $\mathrm{d}\Omega$ along the incidence angle ϕ and absorbed by a volume element ($j = 1, 2, \ldots, N$), on the lower ($j = 0$) or upper ($j = N+1$) boundary, can be written as

$$Q_{\phi N+1,j} = \cos\phi\, \mathrm{d}\Omega \varepsilon_L n_L^2 I_b(T_L) D_{\phi N+1,j} \tag{6}$$

The radiation distribution factor $D_{\phi N+1,j}$ is the fraction of the total radiation emitted from the upper boundary surface in a solid angle $\mathrm{d}\Omega$ that is absorbed by element j. The radiation distribution factor $D_{\phi N+1,j}$ is determined using the Monte Carlo curved ray-tracing method. Similarly, the radiant power emitted by element j and absorbed by the upper surface in a solid angle $\mathrm{d}\Omega$ along the angle ϕ can be written as

$$Q_{j,\phi N+1} = 4\pi k_a \Delta z_j n_j^2 I_b(T_j) D_{j,\phi N+1}$$
$$j = 1, 2, \ldots, N \tag{7a}$$

$$Q_{j,\phi N+1} = \varepsilon_j \pi n_j^2 I_b(T_j) D_{j,\phi N+1}$$
$$j = 0 \quad \text{or} \quad j = N+1 \tag{7b}$$

where Δz_j is the thickness of the volume element j, and the radiation distribution factor $D_{j,\phi N+1}$ is the fraction of the total radiation emitted from element j that absorbed by the upper boundary in a solid angle $\mathrm{d}\Omega$ along the angle ϕ.

According to the reciprocity of the radiation distribution factor,[28] we have

$$\cos\phi\, \mathrm{d}\Omega \varepsilon_L n_L^2 D_{\phi N+1,j} = 4\pi k_a \Delta z_j n_j^2 D_{j,\phi N+1}$$
$$j = 1, 2, \ldots, N \tag{8a}$$

$$\cos\phi\, \mathrm{d}\Omega \varepsilon_L n_L^2 D_{\phi N+1,j} = \varepsilon_j \pi n_j^2 D_{j,\phi N+1}$$
$$j = 0 \quad \text{or} \quad j = N+1 \tag{8b}$$

For backward Monte Carlo simulation, radiant energy emerging from the slab and absorbed by the upper boundary surface in a solid angle $\mathrm{d}\Omega$ along the angle ϕ is calculated by

$$Q_L = \sum_{j=0}^{N+1} \cos\phi\, \mathrm{d}\Omega \varepsilon_L n_L^2 D_{\phi N+1,j} I_b(T_j) \tag{9}$$

and the exit radiation intensity $I_L(\phi)$ at the upper boundary is given as

$$I_L(\phi) = \frac{Q_L}{\varepsilon_L \cos\phi\, \mathrm{d}\Omega} = \sum_{j=0}^{N+1} n_L^2 D_{\phi N+1,j} I_b(T_j) \tag{10}$$

Similarly, the exit radiation intensity $I_0(\phi)$ at the lower boundary is computed by

$$I_0(\phi) = \sum_{j=0}^{N+1} n_0^2 D_{\phi 0,j} I_b(T_j) \tag{11}$$

Here, the radiation distribution factor $D_{\phi 0,j}$ is the fraction of the total radiation emitted from the lower boundary surface in a solid angle $\mathrm{d}\Omega$ that is absorbed by element j. After the radiation distribution factors $D_{\phi 0,j}$ and $D_{\phi N+1,j}$ are solved by the Monte Carlo curved ray-tracing method, the direct problem can be solved by Eqs. (10) and (11).

IV. Inverse Problem

The source term involving the fourth power of the temperature is presented as an Mth polynomial in the dimensionless axis coordinate $Z = z/z_L$,

$$I_b(Z) = \frac{\sigma T^4(Z)}{\pi} = \sum_{m=0}^{M} a_m Z^m \tag{12}$$

Using the known temperature data of the boundary surfaces, the source term can be rewritten as

$$I_b(Z) = I_b(0) + \sum_{m=1}^{M-1} a_m Z^m + \left[I_b(1) - I_b(0) - \sum_{m=1}^{M-1} a_m \right] Z^M \tag{13}$$

where a_m is the coefficient of expansion. The inverse radiation problem can be formulated as an optimization problem. We wish to minimize the function

$$\Gamma(\boldsymbol{a}) = \sum_{\mu_i < 0} [I_0(\phi_i; \boldsymbol{a}) - X(\phi_i)]^2 + \sum_{\mu_i > 0} [I_L(\phi_i; \boldsymbol{a}) - Y(\phi_i)]^2 \tag{14}$$

where X and Y are the measured exit radiation intensities at the boundaries of $Z = 0$ and $Z = 1$, respectively; and $I_0(\phi_i; \boldsymbol{a})$ and $I_L(\phi_i; \boldsymbol{a})$ are the estimated exit radiation intensities at $Z = 0$ and $Z = 1$, respectively, for an estimated vector $\boldsymbol{a} = (a_1, a_2, \ldots, a_{M-1})^T$. Mathematically, the inverse problem belongs to the class of problems called ill-posed problems. To overcome such difficulties, we consider the least-squares norm modified by addition of a zeroth-order regularization term. In the regularization procedure for the inverse radiation problem considered here, an augmented sum of squares function is minimized:

$$J(\boldsymbol{a}) = \sum_{\mu_i < 0} [I_0(\phi_i; \boldsymbol{a}) - X(\phi_i)]^2 + \sum_{\mu_i > 0} [I_L(\phi_i; \boldsymbol{a}) - Y(\phi_i)]^2 + \gamma \sum_{m=1}^{M-1} a_m \tag{15}$$

Here, γ is a regularization parameter, which is determined by the iteration

$$\gamma^{k+1} = \gamma_0 \Gamma(\boldsymbol{a}^k) \left[\sum_{\mu_i < 0} X^2(\phi_i) + \sum_{\mu_i > 0} Y^2(\phi_i) \right]^{-1} \tag{16}$$

where superscript k denotes the kth iteration and γ_0 is the initial value of the regularization parameter, which is set as $\gamma_0 = 0.1$ in this Note.

The sensitivity coefficients $\partial I_0/\partial a_m$ can be determined by differentiating Eqs. (10) and (11):

$$\frac{\partial I_0(\phi)}{\partial a_m} = \sum_{j=0}^{N+1} n_0^2 D_{\phi 0,j} Z_j^m, \qquad \frac{\partial I_L(\phi)}{\partial a_m} = \sum_{j=0}^{N+1} n_L^2 D_{\phi N+1,j} Z_j^m \tag{17}$$

We use the conjugate gradient method to determine the unknown source term. The stopping criterion of iteration is selected in the following manner:

$$|\Gamma(\boldsymbol{a}^{k+1}) - \Gamma(\boldsymbol{a}^k)|/\Gamma(\boldsymbol{a}^k) < \delta \tag{18}$$

where δ is a small specified positive number.

V. Results and Discussion

To demonstrate the effects of measurement errors on the predicted source term, we consider the random errors. The simulated measured exit radiation intensities with random errors are obtained by adding normally distributed errors into the exact exit radiation intensities as

$$[X(\phi_i)]_{\text{measured}} = [X(\phi_i)]_{\text{exact}} + \sigma_X \varsigma, \qquad \mu_i < 0 \quad (19a)$$

$$[Y(\phi_i)]_{\text{measured}} = [Y(\phi_i)]_{\text{exact}} + \sigma_Y \varsigma, \qquad \mu_i > 0 \quad (19b)$$

Here, ς is a normally distributed random variable with zero mean and unit standard deviation. The standard deviations of measured radiation intensities σ_X and σ_Y, for a $\eta\%$ measured error at 99% confidence, are determined as

$$\sigma_X = \frac{[X(\phi_i)]_{\text{exact}} \times \eta\%}{2.576}, \qquad \sigma_Y = \frac{[Y(\phi_i)]_{\text{exact}} \times \eta\%}{2.576} \quad (20)$$

where X_{exact} and Y_{exact} are the exact exit radiation. For the sake of comparison, the relative error of the estimate for the source term is defined as

$$E_{\text{rel}} = \left\{ \int_0^1 [I_{b,\text{estimated}}(Z) - I_{b,\text{exact}}(Z)]^2 \, \mathrm{d}Z \right\}^{\frac{1}{2}} \Bigg/ \int_0^1 I_{b,\text{exact}}(Z) \, \mathrm{d}Z \quad (21)$$

Consider a source term expressed as

$$I_b(Z) = 0.2 + 20Z + 44Z^2 - 128Z^3 + 64Z^4 \ \text{W/cm}^2 \quad (22)$$

The optical thickness of the slab is assumed to be $\tau_L = k_a z_L = 1.0$. We use polynomials of degree 4 to approach the source term profile. The slab is divided into 50 sublayers. To ensure the accuracy of calculation, 10^7 energy bundles are used for the calculation of every radiation distribution factor. In the following analysis, six different angles at each boundary surface are selected to measure the exit radiation intensities. For the case of $n_0 = 1.3$, $n_L = 1.7$, $\varepsilon_0 = 1.0$, $\varepsilon_L = 1.0$, and $\eta = 0$. With no measurement errors, the estimated values of the source term are in excellent agreement with the exact source term. The relative error of the estimation for the source term E_{rel} is less than 0.91%.

In many situations, the refractive index is assumed to be constant. Figure 2 shows the source terms estimated by inverse analysis with the assumption of a constant refractive index in the case of $\varepsilon_0 = 1.0$, $\varepsilon_L = 1.0$ and $\eta = 0$. It can be seen that omitting the effects of the variable spatial refractive index will result in large errors of the estimate for the source term profile, even for a small gradient of the refractive index. Figure 3 shows the distribution of exit radiation intensity at boundary surfaces for five different gradients of the refractive index. With the increase of the refractive index gradient, the difference between exit radiation intensity calculated by considering the refractive index gradient and that calculated under the assumption of constant refractive index increases quickly. Even if the refractive index gradient is small (0.1), the difference is also observable. This is why omitting the effects of the variable spatial refractive index will result in large errors of the estimate, even for a small gradient of the refractive index.

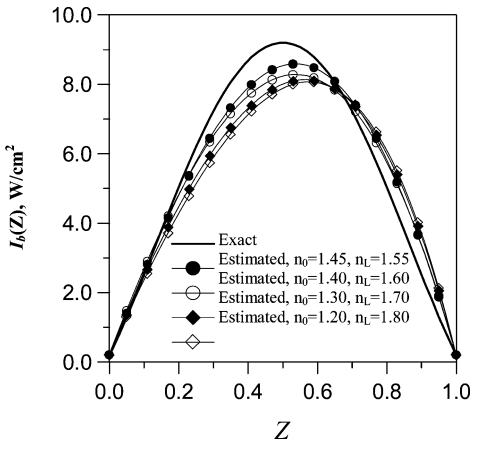

Fig. 2 Source terms estimated by inverse analysis with the assumption of constant refractive index in the case $\varepsilon_0 = 1.0$, $\varepsilon_L = 1.0$, and $\eta = 0$.

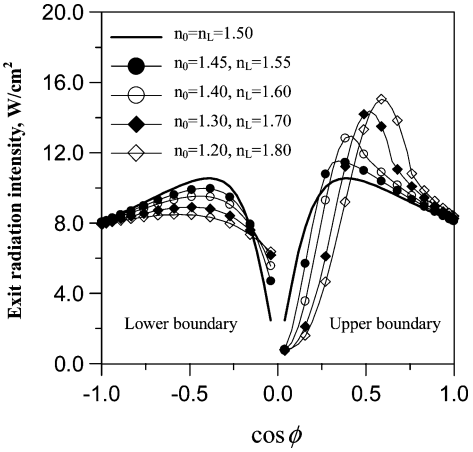

Fig. 3 Distribution of exit radiation intensity at boundary surfaces for five different gradients of refractive index in the case $\varepsilon_0 = 1.0$ and $\varepsilon_L = 1.0$.

The simulated exit radiation intensity measurements containing random errors of $\eta = 5\%$ and 10% are used to estimate the source term profiles in the case $n_0 = 1.2$, $n_L = 1.8$, $\varepsilon_0 = 1.0$, and $\varepsilon_L = 1.0$. The results of 20 random samples are obtained. The relative errors of the source term estimate are within 6% for the case of $\eta = 5\%$ and 10% for the case of $\eta = 10\%$. When the magnitude of measurement errors is increased, the accuracy of the estimate will decrease. Even in the case $\eta = 10\%$, the reconstruction for the source term is good. If the gradient of the refractive index is omitted, even in the case $\eta = 5\%$, the estimated results for the source term profile are bad, and the relative error of the source term estimate is up to 18%.

VI. Conclusions

An inverse analysis is presented for the source term for a semitransparent slab with variable spatial refractive index from the knowledge of the exit radiation intensities at the boundary surface. A backward Monte Carlo curved ray-tracing method based on the radiation distribution factor is used to solve the radiative transfer equation. The inverse problem is formulated as an optimization problem and solved using the conjugate gradient method. The results show that the profiles of the source term can be estimated accurately, even with noisy data. Because the distribution of exit radiation intensities at boundary surfaces changes quickly with the refractive index gradient, omitting the effects of the variable spatial refractive index will result in large errors of the estimate for the source term profile, even for a small gradient of the refractive index.

Acknowledgments

The support of this work by the National Science Foundation of China (50336010) is gratefully acknowledged.

References

[1]Li, H. Y., and Ozisik, M. N., "Identification of the Temperature Profile in an Absorbing, Emitting, and Isotropically Scattering Medium by Inverse Analysis," *Journal of Heat Transfer*, Vol. 114, No. 4, 1992, pp. 1060–1063.

[2]Siewert, C. E., "An Inverse Source Problem in Radiative Transfer," *Journal of Quantitative Spectroscopy and Radiative Transfer*, Vol. 50, No. 6, 1993, pp. 603–609.

[3]Siewert, C. E., "A Radiative-Transfer Inverse-Source Problem for a Sphere," *Journal of Quantitative Spectroscopy and Radiative Transfer*, Vol. 52, No. 2, 1994, pp. 157–160.

[4]Li, H. Y., "Estimation of the Temperature Profile in a Cylindrical Medium by Inverse Analysis," *Journal of Quantitative Spectroscopy and Radiative Transfer*, Vol. 52, No. 6, 1994, pp. 755–764.

[5]Li, H. Y., "Inverse Radiation Problem in Two-Dimensional Rectangular Media," *Journal of Thermophysics and Heat Transfer*, Vol. 11, No. 4, 1997, pp. 556–561.

[6]Li, H. Y., "An Inverse Source Problem in Radiative Transfer for Spherical Media," *Numerical Heat Transfer, Part B*, Vol. 31, No. 2, 1997, pp. 251–260.

[7]Liu, L. H., Tan, H. P., and Yu, Q. Z., "Inverse Radiation Problem of Temperature Field in Three-Dimensional Rectangular Furnaces," *International Communications in Heat and Mass Transfer*, Vol. 26, No. 2, 1999, pp. 239–248.

[8]Liu, L. H., Tan, H. P., and Yu, Q. Z., "Inverse Radiation Problem in One-Dimensional Semitransparent Plane-Parallel Media with Opaque and Specularly Reflecting Boundaries," *Journal of Quantitative Spectroscopy and Radiative Transfer*, Vol. 64, No. 4, 2000, pp. 395–407.

[9]Liu, L. H., Tan, H. P., and Yu, Q. Z., "Inverse Radiation Problem in Axisymmetric Free Flames," *Journal of Thermophysics and Heat Transfer*, Vol. 14, No. 3, 2000, pp. 450–452.

[10]Yousefian, Y., and Lallemand, M., "Inverse Radiative Analysis of High-Resolution Infrared Emission Data for Temperature and Species Profiles Recoveries in Axisymmetric Semitransparent Media," *Journal of Quantitative Spectroscopy and Radiative Transfer*, Vol. 60, No. 6, 1998, pp. 921–931.

[11]Yousefian, Y., Sakami, M., and Lallemand, M., "Recovery of Temperature and Species Concentration Profiles in Flames Using Low-Resolution Infrared Spectroscopy," *Journal of Heat Transfer*, Vol. 121, No. 2, 1999, pp. 268–279.

[12]Solomon, P. R., Best, P. E., Carangelo, R. M., Markham, J. R., and Chien, P. L., "FT-IR Emission/Transmission Spectroscopy for In Situ Combustion Diagnostics," *Proceedings of the Twenty-First International Symposium on Combustion*, edited by H. B. Palmer, Combustion Inst., Pittsburgh, PA, 1986, pp. 1763–1771.

[13]Best, P. E., Chien, P. L., Carangelo, R. M., Solomon, P. R., Danchak, M., and Ilovici, I., "Tomographic Reconstruction of FT-IR Emission and Transmission Spectra in a Sooting Laminar Diffusion Flame: Species Concentration and Temperatures," *Combustion and Flame*, Vol. 85, No. 3–4, 1991, pp. 309–318.

[14]Siegel, R., and Spuckler, C. M., "Variable Refractive Index Effects on Radiation in Semitransparent Scattering Multilayered Regions," *Journal of Thermophysics and Heat Transfer*, Vol. 7, No. 4, 1993, pp. 624–630.

[15]Siegel, R., and Spuckler, C. M., "Refractive Index Effects on Radiation in an Absorbing, Emitting, and Scattering Laminated Layer," *Journal of Heat Transfer*, Vol. 115, No. 1, 1993, pp. 194–200.

[16]Ben Abdallah, P., and Le Dez, V., "Thermal Field Inside an Absorbing–Emitting Semitransparent Slab at Radiative Equilibrium with Variable Spatial Refractive Index," *Journal of Quantitative Spectroscopy and Radiative Transfer*, Vol. 65, No. 4, 2000, pp. 595–608.

[17]Ben Abdallah, P., and Le Dez, V., "Thermal Emission of a Two-Dimensional Rectangular Cavity with Spatial Affine Refractive Index," *Journal of Quantitative Spectroscopy and Radiative Transfer*, Vol. 66, No. 6, 2000, pp. 555–569.

[18]Ben Abdallah, P., and Le Dez, V., "Radiative Flux Field Inside Absorbing-Emitting Semitransparent Slab with Variable Spatial Refractive Index at Radiative Conductive Coupling," *Journal of Quantitative Spectroscopy and Radiative Transfer*, Vol. 67, No. 2, 2000, pp. 125–137.

[19]Ben Abdallah, P., and Le Dez, V., "Thermal Emission of a Semitransparent Slab with Variable Spatial Refractive Index," *Journal of Quantitative Spectroscopy and Radiative Transfer*, Vol. 67, No. 3, 2000, pp. 185–198.

[20]Liu, L. H., "Discrete Curved Ray-Tracing Method for Radiative Transfer in an Absorbing–Emitting Semitransparent Slab with Variable Spatial Refractive Index," *Journal of Quantitative Spectroscopy and Radiative Transfer*, Vol. 83, No. 2, 2004, pp. 223–228.

[21]Lemonnier, D., and Le Dez, V., "Discrete Ordinates Solution of Radiative Transfer Across a Slab with Variable Refractive Index," *Journal of Quantitative Spectroscopy and Radiative Transfer*, Vol. 73, No. 2–5, 2002, pp. 195–204.

[22]Huang, Y., Xia, X. L., and Tan, H. P., "Radiative Intensity Solution and Thermal Emission Analysis of a Semitransparent Medium Layer with a Sinusoidal Refractive Index," *Journal of Quantitative Spectroscopy and Radiative Transfer*, Vol. 74, No. 2, 2002, pp. 217–233.

[23]Huang, Y., Xia, X. L., and Tan, H. P., "Temperature Field of Radiative Equilibrium in a Semitransparent Slab with a Linear Refractive Index and Gray Walls," *Journal of Quantitative Spectroscopy and Radiative Transfer*, Vol. 74, No. 2, 2002, pp. 249–261.

[24]Liu, L. H., Tan, H. P., and Yu, Q. Z., "Temperature Distributions in an Absorbing–Emitting–Scattering Semitransparent Slab with Variable Spatial Refractive Index," *International Journal of Heat and Mass Transfer*, Vol. 46, No. 15, 2003, pp. 2917–2920.

[25]Walters, D. V., and Buckius, R. O., "Rigorous Development for Radiation Heat Transfer in Nonhomogeneous Absorbing, Emitting and Scattering Media," *International Journal of Heat and Mass Transfer*, Vol. 35, No. 12, 1992, pp. 3323–3333.

[26]Modest, M. F., "Backward Monte Carlo Simulations in Radiative Heat Transfer," *Journal of Heat Transfer*, Vol. 125, No. 1, 2003, pp. 57–62.

[27]Liu, L. H., "Backward Monte Carlo Method Based on Radiation Distribution Factor," *Journal of Thermophysics and Heat Transfer*, Vol. 18, No. 1, 2004, pp. 151–153.

[28]Mahan, J. R., *Radiation Heat Transfer*, Wiley, New York, 2002, pp. 390–408.

Turbulator Effects on Heat Transfer in Fan-Driven Flows

Tzeng-Yuan Chen* and Min-Ji Suen†
Tamkang University, Taipei County 251, Taiwan, Republic of China

Nomenclature

A	=	heat transfer surface area, cm
D	=	duct hydraulic diameter, cm
H	=	vertical height of the delta-wing turbulator, cm
h	=	convective heat transfer coefficient, W/(m^2 · K)
k	=	thermal conductivity of the air, W/(m · K)
Nu	=	Nusselt number
Q_{in}	=	power input to the heat transfer surface, W
Q_{loss}	=	conduction and radiation losses, W
T_0	=	air inlet temperature, °C
T_w	=	heat transfer surface temperature, °C
X	=	axial spatial coordinate, cm

Introduction

THIS research effort investigated the effects of delta-wing turbulators on heat transfer in fan-driven swirling flow, and the results were compared with those in uniform flow. The studies of heat transfer augmentation in uniform flow by various types of turbulators, including rib turbulators, arrays of pin fins, wing-type turbulators, shaped roughness elements, arrays of dimples, and so on, have received much attention in the past. For example, Eibeck and Eaton[1] examined the heat transfer effects of a longitudinal vortex embedded in a turbulent boundary layer for various vortex circulations. Tiggelbeck et al.[2] conducted experimental investigations on heat transfer enhancement and induced drag using delta wings, rectangular wings, delta winglets, and rectangular winglets in channel flows. Biswas et al.[3] studied the effects of delta-wing and winglet vortex generators on heat transfer in a channel flow. Ligrani et al.[4] investigated the flow structure and local Nusselt number variations in a channel with a dimpled surface on one wall, both with and without protrusions on the opposite walls. These studies have indicated that turbulators in uniform flow have substantial effects on heat transfer augmentation.

Received 2 January 2003; revision received 20 January 2004; accepted for publication 2 February 2004.

*Associate Professor, Department of Aerospace Engineering, 151 Yingchuan Road.

†Graduate Research Assistant, Department of Aerospace Engineering.